

Domain Adaptation based Interpretable Image Emotion Recognition using Facial Expression Recognition

PUNEET KUMAR and BALASUBRAMANIAN RAMAN, Indian Institute of Technology Roorkee, India

A domain adaptation technique has been proposed in this paper to identify the emotions in generic images containing facial & non-facial objects and non-human components. It addresses the challenge of the insufficient availability of pre-trained models and well-annotated datasets for image emotion recognition (IER). It starts with proposing a facial emotion recognition (FER) system and then moves on to adapting it for image emotion recognition. First, a deep-learning-based FER system has been proposed that classifies a given facial image into discrete emotion classes. Further, an image recognition system has been proposed that adapts the proposed FER system to recognize the emotions portrayed by images using domain adaptation. It classifies the generic images into 'happy,' 'sad,' 'hate,' and 'anger' classes. A novel interpretability approach, Divide and Conquer based Shap (DnCShap), has also been proposed to interpret the highly relevant visual features for emotion recognition. The proposed system's architecture has been decided through ablation studies, and the experiments are conducted on four FER and four IER datasets. The proposed IER system has shown an emotion classification accuracy of 59.61% for the IAPSA dataset, 57.83% for the ArtPhoto dataset, 67.93% for the FI dataset, and 55.13% for the EMOTIC dataset. The important visual features leading to a particular emotion class have been identified, and the embedding plots for various emotion classes have been analyzed to explain the proposed system's predictions.

CCS Concepts: • **Information systems** → **Sentiment analysis**; *Clustering and classification*; *Information systems applications*.

Additional Key Words and Phrases: Interpretable AI, Transfer Learning, Domain Adaptation, Image Emotion Recognition, Discrepancy Loss

ACM Reference Format:

Puneet Kumar and Balasubramanian Raman. 2022. Domain Adaptation based Interpretable Image Emotion Recognition using Facial Expression Recognition. *ACM Trans. Multimedia Comput. Commun. Appl.* 1, 1, Article 1 (November 2022), 19 pages. <https://doi.org/10.1145/1122445.1122456>

1 INTRODUCTION

Humans predominantly portray emotion-related information visually. The images and videos portraying various emotions may contain facial contents, human activities, different backgrounds, and non-human objects. There is a need to develop computational systems that can identify the emotional information expressed in them. These systems study people's emotional responses to visual information [16], and they find their usage in animation, gaming, marketing, entertainment, graphics, and lie detection [16, 19]. The semantic-level IER analysis [26] has been explored by the researchers; however, affective level analysis is more difficult [19, 28, 34]. The recent progress of deep learning has caused enormous performance boost for image recognition and object classification [21, 26].

Authors' address: Puneet Kumar, pkumar99@cs.iitr.ac.in; Balasubramanian Raman, bala@cs.iitr.ac.in, Indian Institute of Technology Roorkee, India, 247667.

Permission to make digital or hard copies of all or part of this work for personal or classroom use is granted without fee provided that copies are not made or distributed for profit or commercial advantage and that copies bear this notice and the full citation on the first page. Copyrights for components of this work owned by others than ACM must be honored. Abstracting with credit is permitted. To copy otherwise, or republish, to post on servers or to redistribute to lists, requires prior specific permission and/or a fee. Request permissions from permissions@acm.org.

© 2022 Association for Computing Machinery.

1551-6857/2022/11-ART1 \$15.00

<https://doi.org/10.1145/1122445.1122456>

Deep learning-based approaches have been successfully used for FER; however, emotion analysis in generic images is a very complex task as they may include human-face, non-facial components, and non-human objects. The emotional expression in images is sometimes attributed to high-level visual features such as background, and facial structure, whereas, sometimes, low-level image features such as texture, edge, color, and shape determine the emotional portrayal in images.

In the context of emotion recognition in the visual domain, FER has been explored extensively [24, 31, 39, 42]. However, FER approaches can not be used for generic images' IER as is. IER does not have sufficient pre-trained models and well-annotated datasets compared to FER. Another challenge associated with IER is human subjectivity in portraying and annotating emotions. The proposed system uses domain adaptation to leverage the advances in FER to perform IER. It formulates the target task of IER as per the source task of FER. Domain adaptation is a special case of transfer learning when the source and target domain contain identical feature space and carry out the same task; however, their data points' distribution is different.

The proposed system classifies an image into discrete categories. It adapts the FER model, which is constructed using VGG16, residual blocks, convolution, max pooling, and dense layers. This main FER model is trained for the FER task using the Adam optimizer. The adapted IER model with the same architecture as the main FER model is simultaneously trained for the IER task. During this process, the discrepancy loss is minimized between the main FER model and the adapted IER model. Training both models using the discrepancy loss enables the adapted IER model to learn the IER domain's distribution. The DnCShap interpretability approach proposed in section 3.4.1 provides more meaningful interpretations by reporting the input features contributing the most towards recognizing a particular emotion class.

The architecture of the proposed IER system and the corresponding domain adaptation strategy have been determined through ablation studies, where various intra-domain and inter-domain adaptation approaches have been explored. The IER experiments on International Affective Picture System Subset a (IAPSa), ArtPhoto, Flickr & Instagram, and The EMOTions In Context (EMOTIC) datasets resulted in emotion recognition accuracies of 59.61%, 57.83%, 67.93%, and 55.13% have been achieved on them, respectively. The feature maps have been computed using the DnCShap technique that identifies the important input features causing the recognition of a particular emotion category.

The contributions of this paper are summarized below.

- (1) A domain-adaptation-based IER system has been proposed to classify generic images containing facial, non-facial, and non-human components into discrete emotion classes.
- (2) A domain adaptation strategy to simultaneously train FER and IER models using discrepancy loss has been proposed that enables the FER models to adapt for IER and learn IER datasets' distribution.
- (3) The DnCShap interpretability technique has been incorporated for IER, which identifies the input features contributing most towards recognizing a particular emotion class.
- (4) A novel strategy to interpret the proposed IER system's layer-by-layer learning and its predictions have also been proposed.

The rest of the manuscript has been organized as follows. Section 2 presents a review of the related research, whereas the proposed system has been discussed in Section 3. Section 4 discusses the implementation details and presents the results. Section 5 concludes the manuscript and highlights the potential advances for future research.

2 RELATED WORK

2.1 Image emotion recognition

Facial expressions are the most predominant ways for the machine perception of emotions. Facial emotion recognition is a well-established and researched area compared to other modalities of emotion analysis. Various methods such as micro-expression analysis, face localization, landmark points' analysis, face registration, shape feature analysis, face segmentation, and eye gaze prediction have been developed for FER [6, 24]. On the contrary, IER has recently started catching researchers' attention. In this context, Kim et al. [19] developed a deep neural-based system that fuses various emotion features from the image, whereas Rao et al. [34] developed hierarchical emotion recognition notations.

2.1.1 Facial expression recognition. Various techniques have been developed for facial expression recognition [1, 13, 31]. The conventional FER approaches extract the features manually and process them. On the other hand, deep learning-based FER methods perform end-to-end analysis without handcrafted feature processing. They also focus on explaining the internal working of the emotion analysis model [45].

Traditional FER approaches: The traditional methods for FER mainly include three phases, i.e., pre-processing, feature extraction, and feature classification [7]. Histogram equalization is the most common approach for pre-processing phase [13, 48] whereas local binary patterns [5], gradients' histograms [15], and Gabor wavelets [2] are used for feature extraction. However, the traditional FER approaches cannot handle the intra-class variations in the input data.

Deep Learning based FER methods: These methods overcome the aforementioned difficulty of handling input data's intra-class variations [49]. To this end, a better FER performance has been demonstrated for the CK dataset using a deep network with zero-bias [18]. Aneja et al. [1] developed a deep FER model for animated images, human faces, and human-to-animation mapping. The attention-based networks have also been used to identify the salient input features for FER [31]. Recently, some work on end-to-end facial emotion recognition and representation has been carried out. For example, Pedro et al. [8] first generated attention feedback through facial image correction and then classified the facial expressions using the feedback.

2.1.2 Generic image emotion recognition. IER was traditionally performed with the help of low-level features, for example, shape, color, and edge [12]. The mid-level features, for example, composition and optical balance, have also been found to add to image aesthetics [16]. In one of the works, S. Zhao et al. [54] used mid-level visual features to perform IER. In another research, the semantic visual content was utilized for the same [28]. The IER approaches are also classified based on emotion categories and dimensions. The dimensional emotion space (DES) approaches [19, 55] utilize arousal and valence to analyze the emotional states. In contrast, the computational results are mapped to discrete emotion classes by the Categorical emotion states (CES) approaches [34, 53, 54]. CES approaches are easier to understand; hence, they are used more often. The proposed system is also a CES-based approach that identifies a given image to have happy, sad, angry, or hateful emotions.

Traditional IER approaches: Conventionally, IER was performed using a feature-based semantic analysis of low-level features (color, edge, and shape) [12]. On the other hand, mid-level features such as composition and optical balance were found to add to image aesthetics [16]. In this direction, Zhao et al. [54] performed mid-level feature-based IER, and Machajdik et al. [28] performed semantic

image content-based emotion analysis. However, the traditional IER approaches are not likely to use all image semantics and mid and low-level features as they use manually crafted features.

Deep Learning based IER methods: The deep learning-based methods extract visual features without manual intervention in an end-to-end fashion. CNN-based transfer learning techniques such as Fine-tuned CNN [52], Feature-based IER [54], Instance Learning-based IER [35] have been used for IER. However, they find it challenging to extract low and mid-level features useful to perform IER precisely [34]. They also face the challenges of insufficient well-annotated large-scale IER datasets and human subjectivity of emotion perception while preparing such datasets. Because of the aforementioned reasons, the existing computer vision models can not perform IER efficiently. They are required to be modified and adapted for IER.

2.2 Transfer Learning and Domain Adaptation for IER

Emotion Recognition has extensively been performed through facial images [11, 31]. The existing approaches mostly use emotional facial features. In this context, Fernandez et al. [8] developed an end-to-end FER network based on the attention model. There are various domain adaptation approaches available in the literature, for example, Feature Augmentation based [25], Feature Transformation based [38], Dictionary method based [41], Reconstruction-based [10], Adversarial-based [9] and Divergence-based [37] Domain Adaptation. The discrepancy loss and classification loss have been used in many typical domain adaptation methods, such as [9, 47].

In this context, a technique to learn the mapping from face images into a representational space using face-similarity measure was presented in FaceNet architecture [39]. However, FER models can not be used for non-facial images' IER as is. They need to be adapted for emotion recognition in generic non-facial images'. In this paper, an IER system has been proposed that adapts the pre-trained FER models. A novel technique for the proposed system's layer-by-layer explanation and to interpret its predictions have also been proposed. The proposed approach also focuses on insufficient IER datasets, IER when facial information is not present in the images, and the incapability of pre-trained convolutional networks to accommodate high, mid, and low visual features together.

2.3 Explainability & Interpretability

Explainability and Interpretability are crucial for trusting AI and machine learning for their applications in emotion recognition [46]. Explainability attempts to describe a model's mechanism leading to a particular output, whereas Interpretability also focuses on the model's design in relation to the output [3]. The approaches to explain a deep learning-based classifier's internal working are yet to be explored for image emotion recognition. Riberio et al. [36] highlighted the importance of explaining the process of the classification models. They proposed an algorithm to explain any classifier's prediction by approximating it locally with an interpretable model and finding which part of the input is responsible for a particular output. In a similar work, Shrikumar et al. [43] proposed a method to decompose the output predictions of a neural network by backpropagating the contributions of all the neurons. However, the approaches mentioned above could not show how the network weights get trained.

3 PROPOSED METHOD

This section proposes a novel approach of transferring the FER model to IER task using domain adaptation.

3.1 Problem formulation

The target task T_i is defined as IER for feature space X' and target domain D_i where $D_i \subset X'$. For source domain D_f and feature space X where $D_f \subset X$, task T_f is defined as FER. The T_i in D_i is to be performed using the information of T_f and D_f . Since D_f and D_i have a different distribution of their data points, i.e., images, we map D_i to the source domain's feature space X . As per Pan et al. [32], it maps to Domain Adaptation as D_f , and D_i perform the same task, have the same feature space and have their data points' different marginal distributions.

3.2 Facial emotion recognition

Figure 1 depicts the proposed FER system's architecture. It contains four residual layers on top of a pre-trained VGG16 [44] network. It consists of five blocks containing two, two, three, three, and three convolutional layers with 64, 128, 256, 512, and 512 channels, respectively.

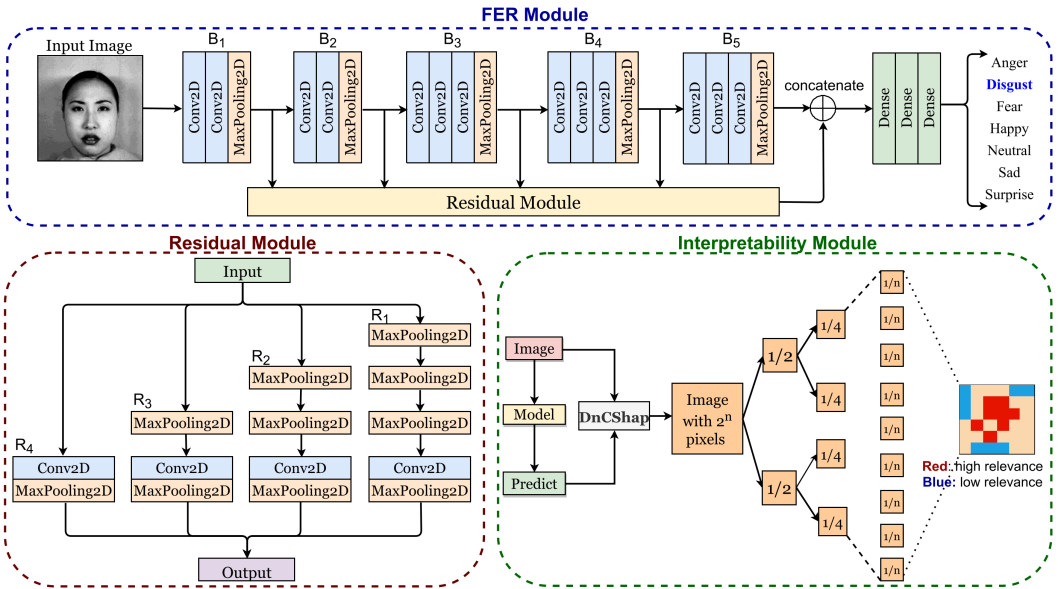


Fig. 1. Architecture of the proposed FER system.

Residual layers follow the FER system's blocks to prevent exploding and vanishing and gradients issues faced by DNNs [14]. The first residual layer contains one convolution layer and four max-pool layers. The second residual layer contains one convolution layer and three max-pool layers. The third residual layer contains one convolution layer and two max-pool layers. The fourth residual layer contains one convolution layer and one max-pool layer. The last block and the Residual Module's output are concatenated and passed to the dense layer after being flattened.

3.3 Image emotion recognition

Figure 2 shows the proposed IER system's architecture that has been decided through the ablation studies. It adapts the target task IER in-line with the source task FER. Its details have been discussed as follows. The proposed system uses the FER model developed in section 3.2, which is built on top of VGG16 by adding the residual blocks along with convolution, max pooling, and dense layers. This main FER model is trained for the FER task using adam optimizer. The adapted IER model with

the same architecture as the main FER model is simultaneously trained for the IER task. During this process, the discrepancy loss is minimized between the main FER model and the adapted IER model.

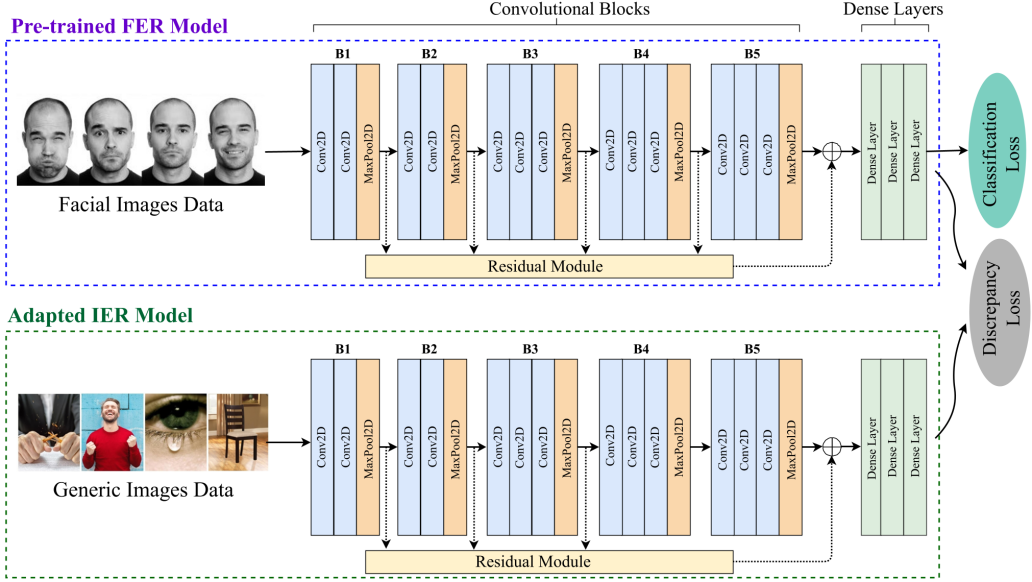


Fig. 2. Architecture of the proposed IER system. The Residual and Explainability modules have been elaborated in Figure 1.

Domain Adaptation scheme: The main FER model and adapted IER model are trained using adam optimizer and cross-entropy loss. In contrast, the discrepancy loss is minimized between them after they get trained for each epoch. The FER and IER domains perform the same task and have identical feature space; however, their data points' marginal distributions are different. Re-training using the discrepancy loss enables the adapted IER model to learn the distribution of the IER domain. The overall loss function described in Eq. 1.

$$\mathcal{L}_{overall} = \mathcal{L}_{classifier} + \mathcal{L}_{discrepancy} + \lambda \|\omega(f_c)\|_2^2 \quad (1)$$

where $\mathcal{L}_{overall}$, $\mathcal{L}_{classifier}$, and $\mathcal{L}_{discrepancy}$ are overall loss, cross-entropy loss and discrepancy loss. The third term is the regularization term, where ω and λ are the weights of the fully connected layers and the regularization weight, which are calculated experimentally by observing the variance in the output. The computation of classifier loss and discrepancy loss has been explained as follows. The cross-entropy loss has been used to find the output probability of the main FER model and the adapted IER model. For an image sample v , distribution p_1 in FER domain and distribution p_2 in IER domain, classifier loss is calculated using Eq. 2.

$$\mathcal{L}_{classifier}(p_1, p_2) = - \sum_{v \in \mathcal{V}} p_1(v) \log(p_2(v)) \quad (2)$$

where v is an image sample whereas p_1 and p_2 denote the actual and predicted distributions of v , respectively. Further, the absolute difference between the two classifiers' probabilistic outputs has

been utilized as discrepancy loss. For the image samples' distribution for FER classifier, p_1 and the predicted distribution for IER classifier, p_2 , the discrepancy loss is calculated as per Eq. 3.

$$\mathcal{L}_{discrepancy}(p_1, p_2) = \frac{1}{K} \sum_{k=1}^{k=K} |o_{1k} - o_{2k}| \quad (3)$$

where o_{1k} and o_{2k} denote the probabilistic outputs for distributions p_1 and p_2 whereas K denotes the number of classes.

3.4 Interpretability of the Predictions

A two-fold Explainability technique has been proposed to explain the working of the proposed method. It first visualizes the important features of the input image responsible for emotion classification. Then, implementing the proposed layer-wise explainability technique results in the intersection matrices and cluster distances.

3.4.1 Feature-wise Explainability. An Interpretability system, Divide and Conquer based SHAP (DnCShap), has been proposed in this section that integrates Divide and Conquer approach into the SHAP method to speed up Shapley values' computation. The shapely values' exact calculation is NP-hard [40], which is approximated by the SHAP algorithm in quadratic time. On the other hand, DnCShap requires linear time to compute the approximated Shapely values.

Calculating Shapley values: The Shapely values' computation has been demonstrated with an example shown in Figure 3. The *Node1* has no feature, *Node4* has two features (f_1 and f_2) and the rest of the nodes contain one feature each (i.e., f_1 and f_2 , respectively). The 'marginal contribution' of a feature differentiates the predictions of two nodes connected by an edge.

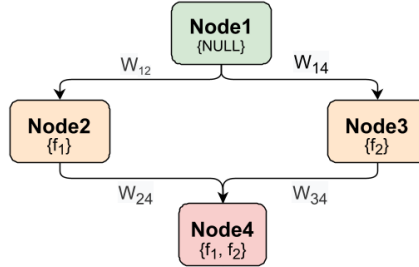


Fig. 3. Illustration of Shapley values calculation.

The feature f_1 's marginal contribution for label c for the model with f_1 feature only is computed as per Eq. 4.

$$MC_{f_1, \{f_1\}} = score_{\{f_1\}} - score_{\{\phi\}} \quad (4)$$

where $score_{\{f_1\}}$ is the prediction for label c using the model with feature f_1 . The overall contribution is computed as per Eq. 5.

$$SHAP_{\{f_i\}} = w_{12} \times MC_{f_i, \{f_i\}} + w_{34} \times MC_{f_i, \{f_i, f_2\}} \quad (5)$$

where w_{12} and w_{34} are the coefficient weights. The coefficient weight, w_i is computed using Eq. 6.

$$w_i = \frac{|S|!(|F| - |S| - 1)!}{|F|!} \quad (6)$$

where $|S|$ denotes no. of features and $|F|$ shows the no. of weights. The values of w_{12} and w_{34} are calculated as per Eq. 6 and Eq. 7 computes the Shapely values.

$$\begin{aligned} w_{12} &= (0!(2 - 0 - 1)!)/(2!) = 1/2 \\ w_{34} &= (1!(2 - 1 - 1)!)/(2!) = 1/2 \\ SHAP_{\{f_i\}} &= \left(\frac{1}{2}\right) \times MC_{f_i, \{f_i\}} + \left(\frac{1}{2}\right) \times MC_{f_i, \{f_i, f_2\}} \end{aligned} \quad (7)$$

Approximating Shapley values: Instead of re-training the model for a varying number of features, we perturb the input to compute the Shapely values. The incorporation of the Divide and Conquer approach enables the Shapely values' computation in linear time as compared to the exponential time required by the existing methods. It recursively divides the image into halves and computes their Shapley values. The difference between average and predicted values give the Shapley values of all features. To compute *score1* and *score2* denoting the Shapley values of two halves obtained by Divide and Conquer, the property shown in Eq. 10 is held true, and *pred_b* and *pred_f* values are chosen accordingly.

For image X with width w and height h , it is divided into two parts x_1, x_2 where width is $w/2$ and height is h . The two parts are considered as different features, and Eq 5 is used to find their Shapley values. The divide and conquer is continuously applied, and Shapely values are found until the image is divided into a pre-specified (hyperparameter) number of parts. The time complexity is of the order of $T(n) = 2T(n/2) + O(1)$, i.e., of the order of $O(n)$, which comes out to be linear time complexity for n number of features.

3.4.2 Layer-wise Explainability. This section proposes a novel technique to explain the predictions of the proposed deep learning-based system. We have defined the term *Intersection Score*, which depicts the correctness of network weights layer by layer. It first visualizes the important features of the input image responsible for emotion classification. The convergence of the emotion clusters is then visualized for various network layers.

The intersection score is calculated using the following steps.

a) For each emotion class i , calculate the principle components (x_i, y_i, z_i) of p^{th} last layer's embedding. For each emotion class i and all three components (x_i, y_i, z_i) , mean m_i and standard deviation $\sigma_{\bar{m}_i}$ are calculated using Eq. 8, where n_i is the number of data points for i^{th} emotion-class and k is the k^{th} data point.

$$\bar{m}_i = \frac{1}{n_i} \sum_{k=1}^{k=n_i} m_k; \sigma_{\bar{m}_i} = \frac{1}{n_i} \sum_{k=1}^{k=n_i} (m_k - \bar{m}_i)^2 \quad (8)$$

$$\forall m \in \{x, y, z\}$$

To get the principle components of a layer's embeddings, first the embedding vector is extracted and flattened. Then the principal component analysis (PCA) procedure is applied, which involves computing eigenvectors; sorting them by decreasing eigenvalues and choosing k eigenvectors with the largest eigenvalues and using this $d \times k$ eigenvector matrix for transformation where d dimensions.

b) For each emotion class i , the range for every principle component is defined using the above parameters with an assumption that most of the values will be within two times the standard deviations of the mean. Range for i^{th} emotion is defined as $[L_i(m), R_i(m)]$ where $L_i(m)$ and $R_i(m)$ are the left and right extreme points of m^{th} component's spread for emotion class i . The extreme points are defined in Eq. 9. The choice of using the double of the standard deviation value to define the range is done under the assumption that the distribution has a symmetric tail on both sides.

$$L_i(m) = \bar{m}_i - 2\sigma_{\bar{m}_i} \quad R_i(m) = \bar{m}_i + 2\sigma_{\bar{m}_i} \quad (9)$$

$$\forall m \in \{x, y, z\}$$

c) The intersection between emotion classes i and j is calculated as per Eq. 10 and denoted as $I_{i,j}(m)$. Here, four emotion classes, i.e., angry, happy, sad, and neutral, are considered.

$$I_{i,j}(m) = \frac{\max\{\min(R_i(m), R_j(m)) - \max(L_i(m), L_j(m)), 0\}}{\max(R_i(m), R_j(m)) - \min(L_i(m), L_j(m))} \quad (10)$$

$$\forall m \in \{x, y, z\}, \quad \forall i, j \in \{1, 2, 3, 4\}$$

Here, $I_{i,j}(m)$ denotes the intersection between the spread of m^{th} component's data for emotion classes i and j .

d) The total intersection between two emotion classes i and j is denoted as $I_{i,j}$. As shown in Eq. 11, it is calculated as the product of all component-wise intersections between emotion classes i and j . The values for $I_{i,j}$ are in the range $[0,1]$. It has a maximum value of one when $i = j$, i.e. when the spread of m^{th} component's data is the same for two emotion classes.

$$I_{i,j} = I_{i,j}(x) * I_{i,j}(y) * I_{i,j}(z) \quad (11)$$

Here, $I_{i,j}$ denotes the total intersection between the emotion classes i and j .

4 IMPLEMENTATION AND EXPERIMENTS

4.1 Datasets

FER Datasets: The following FER datasets have been used.

- *FER13* [4]: This dataset includes 35,887 emotion labeled images with variations such as facial occlusions, and incomplete faces.
- *FERG* [1]: It consists of 55,767 annotated and animated faces from six characters, along with emotion labels.
- *JAFFE* [17]: It includes Japanese female models' 213 images portrayed along with different facial expressions.
- *CK+* [27]: This dataset contains 123 objects' 927 images portrayed along with different emotions.

IER Datasets: The following IER datasets have been used.

- *IAPSa* dataset [30] - The subset A of the IAPS dataset, i.e., IAPSa dataset, has been prepared by Mikels et al. [30] by taking 395 images and mapping their arousal and valence values to discrete emotion categories.
- *ArtPhoto* dataset [28] - It contains 806 art photos whose emotions are labeled by the artists who prepared the photos.
- *Flicker & Instagram (FI)* dataset [52] - It contains 23,308 images collected by You et al. [52] from Flickr and Instagram and labelled with discrete emotion categories.
- *EMOTIC* dataset [20] - It contains the images involving people in various background and contexts. The images are labeled with continuous dimensions and discrete categories.

4.1.1 Training strategy and hyperparameter setting. We have considered 'happy,' 'anger,' 'hate,' and 'sad' classes as these are the common emotion classes considered by the existing methods. The model training is performed using training-testing data split of 80% and 20%, 5-fold cross-validation, a batch size of 16, learning rate of 8×10^{-5} to 8×10^{-4} for up to 100 epochs. The FER and IER models were first trained using cross-entropy loss and then trained together using the discrepancy loss, whereas the adam optimizer was used for both networks. The emotion classes have been merged and re-labeled as per Plutchik's emotion wheel [33]. The 'contentment' and 'amusement' labeled samples are re-labeled as 'happiness,' whereas the 'disgust' labeled samples are merged with the sample having 'hate' label.

4.1.2 Ablation studies. This section discusses the experimental studies performed to determine the appropriate domain adaptation approach.

a) Inter-modality domain adaptation: This trial transforms the visual information into textual and performs the emotion recognition task. This transformation has been performed using image captions generated using an attention-based captioning system [50]. Following this, a pre-trained Text Emotion Recognition (TER) model [23] has been re-trained using these captions, and TER has been performed. The predicted TER labels have been considered the IER labels because the images and captions have one-to-one relations as they verbalize the same information visually and textually. The adapted TER model showed 33.89% accuracy on being tested without re-training on image captions. On the other hand, re-training it with image captions demonstrated 53.07% accuracy. The above-described approach has been implemented in Baseline#4.

b) Intra-modality adaptation: The datasets and pre-trained models for visual object recognition and FER tasks are more abundant. The following approaches have been considered to leverage them for IER.

- The pre-trained object recognition models such as AlexNet, ResNet, and VGG16 were used for IER without re-training. However, it resulted in poor performance of around 30% emotion recognition accuracy.
- The pre-trained FER models were trained further and used for recognizing emotions in images using transfer learning. Taking inspiration from the existing feature transformation-based domain adaptation approaches [38], we have mixed a fraction of IER data with FER data while training the FER model proposed in section 3.2. It enables the FER model to learn the distribution of IER data gradually. Table 1 shows the IER performance on mixing a fraction of IER data along with FER data to train the FER models and test them for IER data.

Table 1. Transformation-based IER experiments. Here, x_i fraction of IER dataset has been mixed with FER dataset to train FER model and test it on IER dataset.

FER dataset	x_1 value for IAPSa IER dataset									
	0.1	0.2	0.3	0.4	0.5	0.6	0.7	0.8	0.9	1.0
FER13	36.68%	39.33%	43.25%	46.65%	47.61%	48.61%	48.16%	49.84%	50.53%	48.95%
FERG	22.53%	26.55%	33.47%	37.02%	40.11%	44.32%	43.19%	43.22%	42.32%	40.67%
JAFFE	28.46%	32.35%	37.40%	41.81%	41.16%	40.53%	39.53%	38.28%	38.62%	39.14%
CK+	34.19%	39.41%	42.78%	43.58%	43.30%	47.74%	49.69%	51.21%	48.11%	49.99%

FER dataset	x_2 value for ArtPhoto IERdataset									
	0.1	0.2	0.3	0.4	0.5	0.6	0.7	0.8	0.9	1.0
FER13	31.74%	38.31%	39.99%	42.61%	45.69%	45.21%	45.13%	45.99%	45.44%	44.98%
FERG	29.91%	36.44%	40.09%	41.13%	43.82%	42.01%	43.49%	42.15%	42.41%	42.86%
JAFFE	37.26%	39.61%	41.96%	45.94%	46.62%	45.61%	45.61%	46.16%	47.25%	47.07%
CK+	30.15%	31.07%	36.16%	39.52%	40.17%	39.42%	41.15%	40.71%	39.14%	40.14%

FER dataset	x_3 value for FI IER dataset									
	0.1	0.2	0.3	0.4	0.5	0.6	0.7	0.8	0.9	1.0
FER13	33.24%	35.92%	41.14%	43.43%	45.55%	47.71%	47.67%	49.96%	45.37%	42.46%
FERG	26.17%	28.48%	30.61%	32.77%	36.17%	39.56%	41.38%	41.15%	40.76%	39.52%
JAFFE	28.43%	29.85%	28.71%	34.18%	39.92%	37.57%	37.13%	35.29%	34.03%	35.57%
CK+	35.29%	38.86%	39.27%	42.96%	44.57%	45.83%	51.39%	57.47%	54.82%	52.27%

FER dataset	x_4 value for EMOTIC IER dataset									
	0.1	0.2	0.3	0.4	0.5	0.6	0.7	0.8	0.9	1.0
FER13	32.24%	40.41%	41.43%	43.59%	44.51%	46.49%	46.29%	45.82%	46.48%	47.17%
FERG	30.39%	38.34%	41.51%	42.53%	44.84%	43.84%	44.48%	43.58%	44.58%	43.61%
JAFFE	35.63%	41.16%	42.63%	43.41%	43.26%	44.15%	46.12%	47.62%	46.53%	46.72%
CK+	34.13%	35.93%	37.49%	41.15%	42.47%	40.48%	41.92%	40.57%	40.59%	39.94%

It has been observed that mixing 40-80% IER data while training the FER model resulted in the best possible IER accuracies by this approach. However, there is a scope to improve it further.

- This approach trains a network for FER and IER simultaneously and minimizes the loss between them during the training. Further, the following networks have been considered while formulating the baseline models and proposed system – AlexNet (Baseline#1), VGG16 (Baseline#2), ResNet (Baseline#3), DeepEmotion [31] (Baseline#5), and the FER model proposed in section 3.2 (Proposed Method). Table 2 summarizes their respective performances. The rationale for choosing DeepEmotion is its state-of-the-art performance for FER, JAFFE and CK+ datasets [29].

Table 2. FER to IER domain adaptation experiments. Here, 'F'→'I' denotes that the IER task on dataset 'I' has been adapted from the FER task on dataset 'F'

IAPSa dataset.					
	FER13→IAPSa	FERG→IAPSa	JAFFE→IAPSa	CK+→IAPSa	All→IAPSa
Baseline#1	39.67%	40.17%	42.43%	42.36%	41.96%
Baseline#2	47.53%	45.68%	45.17%	47.09%	48.53%
Baseline#3	46.89%	46.26%	44.31%	47.16%	47.93%
Baseline#4	53.54%	51.52%	50.29%	52.72%	49.48%
Baseline#5	57.06%	52.29%	53.51%	57.37%	56.43%
<i>Proposed</i>	56.14%	48.63%	51.36%	59.61%	58.93%

ArtPhoto dataset.					
	FER13→ArtPhoto	FERG→ArtPhoto	JAFFE→ArtPhoto	CK+→ArtPhoto	All→ArtPhoto
Baseline#1	45.61%	43.51%	44.76%	46.07%	46.53%
Baseline#2	50.17%	48.35%	49.47%	48.46%	50.26%
Baseline#3	51.82%	49.96%	50.84%	50.83%	51.16%
Baseline#4	47.37%	40.16%	45.46%	49.96%	42.43%
Baseline#5	54.16%	52.71%	55.51%	54.37%	51.27%
<i>Proposed</i>	50.53%	49.47%	57.83%	50.34%	56.96%

FI dataset.					
	FER13→FI	FERG→FI	JAFFE→FI	CK+→FI	All→FI
Baseline#1	56.72%	51.82%	52.17%	54.29%	57.66%
Baseline#2	59.38%	56.46%	54.05%	58.53%	57.36%
Baseline#3	58.24%	54.28%	50.11%	60.81%	56.32%
Baseline#4	59.17%	58.74%	52.82%	57.61%	51.61%
Baseline#5	61.62%	60.37%	62.75%	63.87%	61.53%
<i>Proposed</i>	60.74%	54.47%	53.72%	67.17%	67.93%

EMOTIC dataset.					
	FER13→EMOTIC	FERG→EMOTIC	JAFFE→EMOTIC	CK+→EMOTIC	All→EMOTIC
Baseline#1	40.61%	39.53%	37.59%	40.54%	40.17%
Baseline#2	44.54%	43.16%	42.36%	40.19%	43.96%
Baseline#3	44.61%	45.46%	40.47%	42.93%	46.34%
Baseline#4	46.89%	40.23%	42.87%	47.72%	41.86%
Baseline#5	49.14%	50.37%	48.48%	52.53%	53.46%
<i>Proposed</i>	53.16%	49.82%	52.97%	50.36%	55.13%

The individual FER datasets and their combination (denoted as ‘All’) have been used during the implementation. In most cases, the experiments combining all FER datasets have performed better than the individual FER datasets.

Overall, simultaneous training of the FER model proposed in section 3.2 on FER and IER datasets resulted in better performance. The proposed system implements it. The baselines and proposed system’s architectures decided per the above ablation studies are summarized as follows.

- **Baseline#1:** It trains AlexNet [22] simultaneously for FER and IER.
- **Baseline#2:** The VGG16 [44] based IER and FER models are implemented and trained using discrepancy loss.
- **Baseline#3:** It trains ResNet [14] models simultaneously for FER and IER.
- **Baseline#4:** It generates the captions for the given images and trains the TER model for emotion recognition. The captions’ emotion labels are considered the images’ labels, as there is a one-to-one mapping between them.
- **Baseline#5:** It adapts a pre-trained FER model, Deep Emotion [31] and re-trains it simultaneously for FER and IER using the discrepancy loss.
- **Proposed system:** The proposed IER system adapts the FER model proposed in section 3.2 using the proposed domain adaptation scheme.

4.2 Results and discussion

4.2.1 Accuracy and confusion matrices. The proposed IER system shows 59.61%, 57.83%, 67.93%, and 55.13% accuracies for IAPSa, ArtPhoto, FI, and EMOTIC datasets, respectively. Figure 4 shows the corresponding confusion matrices.

4.2.2 Comparison with existing methods. Table 3 compares the results of the proposed IER system with the existing methods and baseline models.

Table 3. Results’ comparison with the existing IER methods and baselines.

Model	IAPSa	ArtPhoto	FI	EMOTIC
Feature-based IER [54]	49.46%	51.72	-	-
Instance Learning [35]	-	-	51.67%	-
Baseline#1	42.51%	46.53%	57.66%	40.61%
Baseline#2	48.53%	50.26%	59.38%	44.54%
Baseline#3	47.93%	51.82%	60.81%	46.34%
Baseline#4	53.54%	49.96%	59.17%	48.89%
Baseline#5	57.37%	55.51%	63.87%	53.46%
<i>Proposed</i>	59.61%	57.83%	67.93%	55.13%

Many IER works [28, 51] are based on the DES and use True Positive Rate (TPR) instead of accuracy. The CES approaches with known accuracy values have been included for results comparison. Moreover, the aforementioned four emotion classes have been considered for the analysis as these are the common classes in various existing IER methods and image datasets with emotion labels.

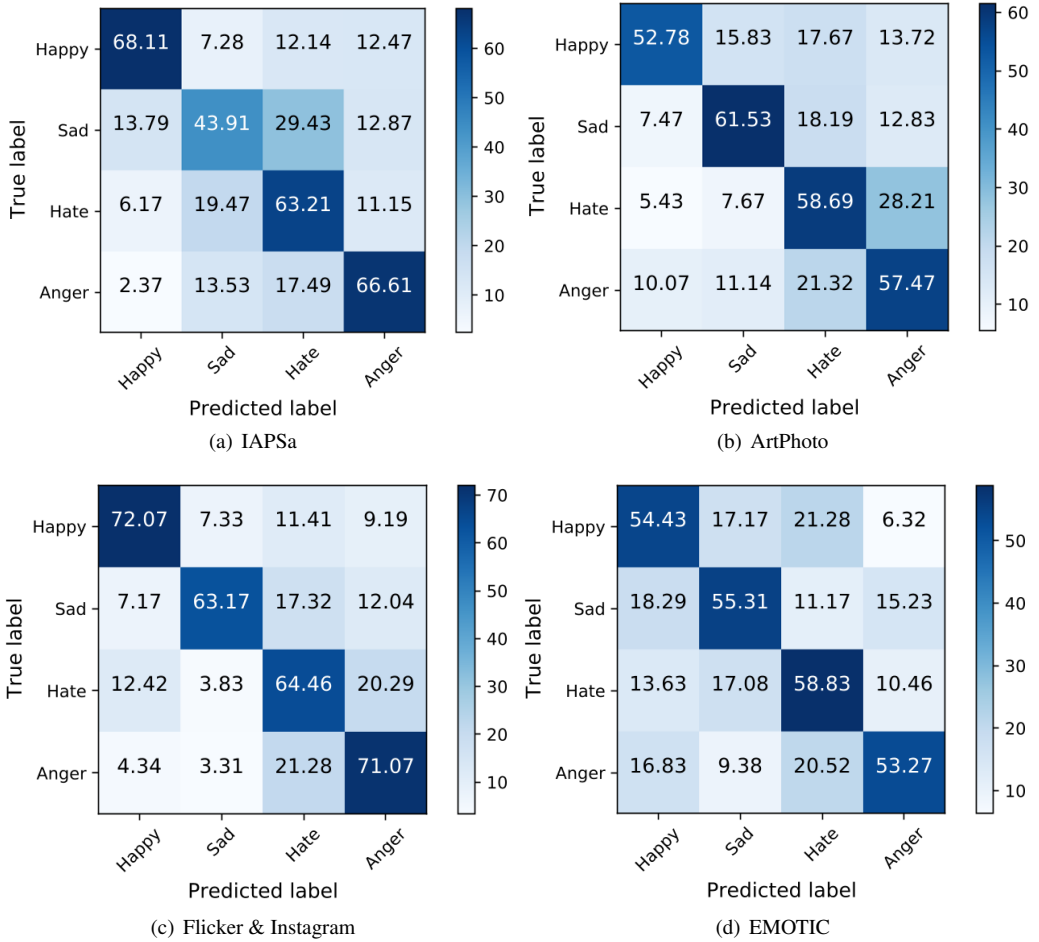


Fig. 4. Confusion matrices for IAPSa, ArtPhoto, FI, and EMOTIC datasets.

4.2.3 Feature-wise Explainability. Figure 5 demonstrates the feature maps for various emotion classes. The feature maps in red highlight the most significant visual features that contribute to emotion recognition.

The visual features associated with particular emotion classes are reported in Figure 5. The facial features have been captured for the images containing human faces. The other relevant areas leading to the classification of a particular emotion class have also been identified for the images without human faces.

4.2.4 Layer-wise Explainability.

In Figure 6, the trained IER model's embeddings are projected on a hyperplane where x , y , and z principle components' spreads are shown along x , y , and z axes for various emotion classes. It can be observed that the spreads separate well as we move from the intermediate to the last layers.

4.2.5 Discussion. As more pre-trained models and labeled large-scale datasets are available for FER, we have proposed a domain adaptation-based system to use them for IER. The proposed

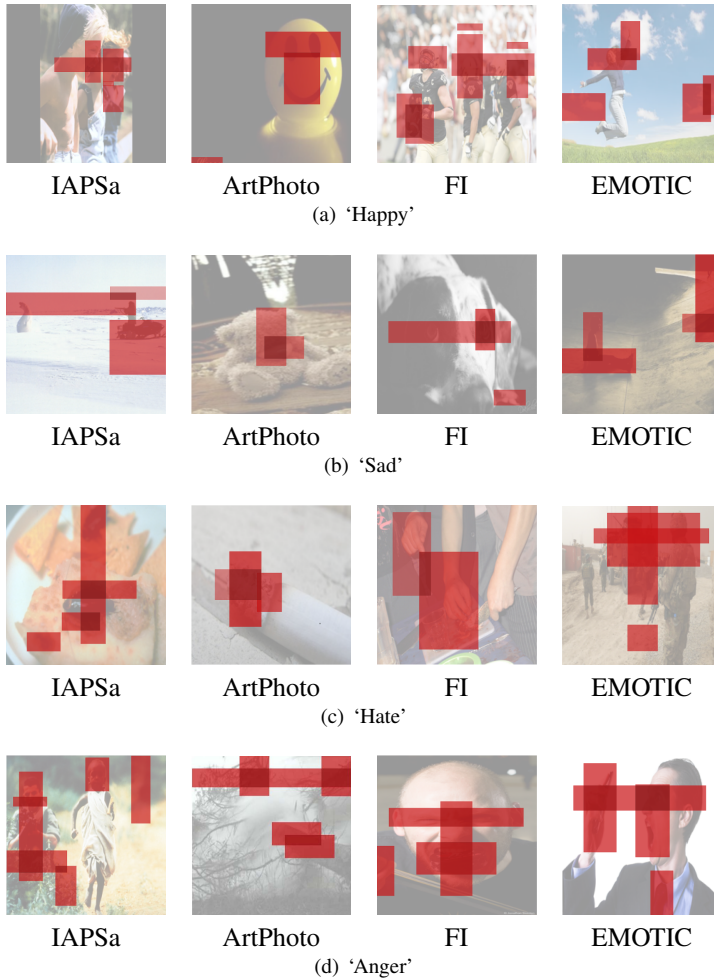


Fig. 5. Feature-wise Explainability for various emotion classes.

system has depicted good IER performance, even for small-scale IER datasets. The proposed domain adaptation approach can solve the problem of lacking datasets and pre-trained models for other research applications. The proposed interpretability approach, DnCSHap, has reported the important features of the image contributing to emotion recognition. As observed from Figure 5, the feature maps for the ‘happy’ and ‘anger’ classes are more precise, whereas those for the ‘sad’ and ‘hate’ classes are more scattered. The identification of important visual features can be further fine-tuned. Moreover, interpretability can be explored for other modalities as well. Transferring the FER model to the IER task is a novel approach that will help solve the problem of lacking large-scale datasets and pre-trained models in the IER field if the method can work well in major scenarios. The interesting Intersection Score helps determine the effectiveness of network layers and brings some interpretability to this deep learning-based system.

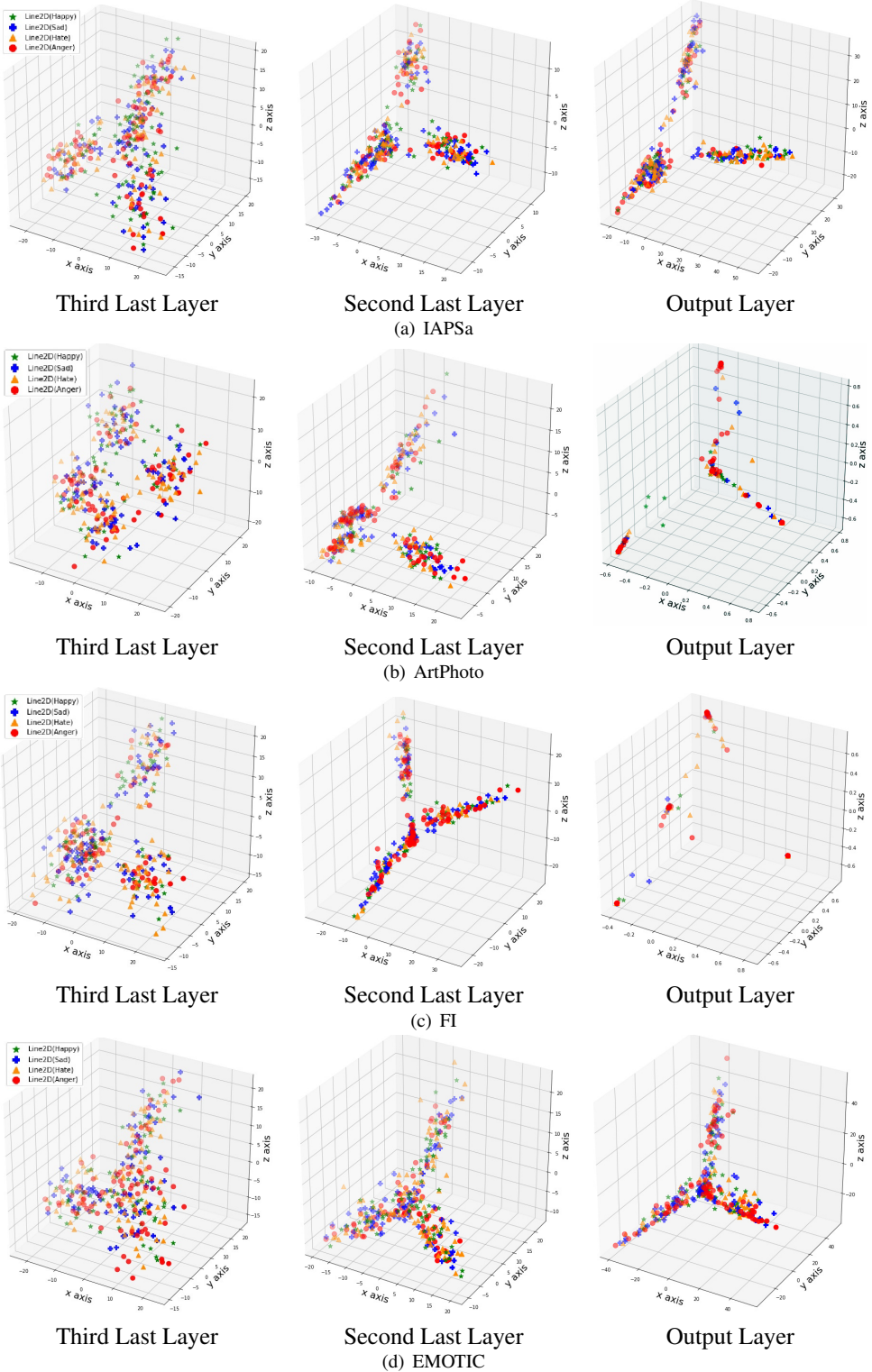


Fig. 6. Layer-wise Explainability for various IER datasets.

5 CONCLUSIONS AND FUTURE WORK

This paper proposes a novel interpretable system for emotion recognition in images containing facial content, human objects, and non-human objects. First, a deep-learning-based FER system based on a pre-trained VGG network and residual learning has been proposed. Further, domain adaptation has been used to learn the distribution of IER datasets along with FER datasets' distribution. The proposed system has been adapted to perform IER by training it for FER and IER simultaneously using the discrepancy loss. The experiments conducted on four FER datasets and four IER datasets produced the expected IER results. A method to interpret the results of the proposed systems has also been proposed. The facial features that are most relevant for emotion recognition have been consistently reported. Future research will explore more transfer learning approaches from various computer vision tasks to image emotion recognition. It is also planned to use the proposed model for computer vision tasks other than emotion recognition. It is also planned to include more emotion classes for IER, for example, disgust, fear, excitement, contentment, and amusement.

ACKNOWLEDGEMENTS

Ministry of Education, Government of INDIA, supported this research with grant number: 1-3146198040.

REFERENCES

- [1] Deepali Aneja, Alex Colburn, Gary Faigin, Linda Shapiro, and Barbara Mones. 2016. Modeling Stylized Character Expressions via Deep Learning. In *The Asian Conference on Computer Vision (ACCV)*. Springer, 136–153.
- [2] Marian Stewart Bartlett, Gwen Littlewort, Mark Frank, Claudia Lainscsek, Ian Fasel, and Javier Movellan. 2005. Recognizing Facial Expression: Machine Learning and Application to Spontaneous Behavior. In *The IEEE/CVF International Conference on Computer Vision and Pattern Recognition (CVPR)*, Vol. 2. 568–573.
- [3] David A Broniatowski et al. 2021. Psychological Foundations of Explainability and Interpretability in Artificial Intelligence. *National Institute of Standards and Technology (NIST)* (2021).
- [4] Pierre-Luc Carrier, Aaron Courville, Ian J Goodfellow, Medhi Mirza, and Yoshua Bengio. 2013. FER-2013 Face Database. *Universit de Montral* (2013).
- [5] Junkai Chen, Zenghai Chen, Zheru Chi, Hong Fu, et al. 2014. Facial Expression Recognition based on Facial Components Detection and HOG Features. In *The International Workshop on Electrical and Computer Engineering Subfields*. 884–888.
- [6] Ciprian Adrian Corneanu, Marc Oliu Simón, Jeffrey F Cohn, and Sergio Escalera Guerrero. 2016. Survey on RGB, 3D, Thermal, and Multimodal Approaches for Facial Expression Recognition: History, Trends, and Affect-related Applications. *IEEE Transactions on Pattern Analysis and Machine Intelligence (TPAMI)* 38, 8 (2016), 1548–1568.
- [7] Marcelo Cossetin et al. 2016. Facial Expression Recognition using a Pairwise Feature Selection and Classification Approach. In *The IEEE International Joint Conference on Neural Networks (IJCNN)*. 5149–5155.
- [8] Pedro D Marrero Fernandez, Fidel A Guerrero Peña, Tsang Ing Ren, and Alexandre Cunha. 2019. FERAtt: Facial Expression Recognition with Attention Net. In *The IEEE/CVF International Conference on Computer Vision and Pattern Recognition-workshops (CVPRw)*. 0–0.
- [9] Yaroslav Ganin and Victor Lempitsky. 2015. Unsupervised domain adaptation by backpropagation. In *International conference on machine learning*. PMLR, 1180–1189.
- [10] Muhammad Ghifary, W Bastiaan Kleijn, Mengjie Zhang, David Balduzzi, and Wen Li. 2016. Deep reconstruction-classification networks for unsupervised domain adaptation. In *European Conference on Computer Vision (ECCV)*. Springer, 597–613.
- [11] Ian J Goodfellow, Dumitru Erhan, Pierre Luc Carrier, Aaron Courville, Mehdi Mirza, Ben Hamner, Will Cukierski, Yichuan Tang, David Thaler, Dong-Hyun Lee, et al. 2015. Challenges in representation learning: A report on three machine learning contests. *Neural Networks* 64 (2015), 59–63.
- [12] Alan Hanjalic. 2006. Extracting Moods from Pictures and Sounds: Towards Personalized TV. *IEEE Signal Processing Magazine* 23, 2 (2006), 90–100.
- [13] SL Happy and Aurobinda Routray. 2014. Automatic Facial Expression Recognition Using Features of Salient Facial Patches. *IEEE Transactions on Affective Computing (TAC)* 6, 1 (2014), 1–12.
- [14] Kaiming He, Xiangyu Zhang, Shaoqing Ren, and Jian Sun. 2016. Deep Residual Learning for Image Recognition. In *IEEE/CVF Conference on Computer Vision and Pattern Recognition (CVPR)*. 770–778.

- [15] Paul VC Hough. 1962. Method and Means for Recognizing Complex Patterns. US Patent 3,069,654.
- [16] Dhiraj Joshi, Ritendra Datta, Elena Fedorovskaya, Quang-Tuan Luong, James Z Wang, Jia Li, and Jiebo Luo. 2011. Aesthetics and Emotions in Images. *IEEE Signal Processing Magazine* 28, 5 (2011), 94–115.
- [17] Miyuki Kamachi, Michael Lyons, and Jiro Gyoba. 1998. The Japanese Female Facial Expression (JAFFE) Database. www.kasrl.org/jaffe.html 21 (1998), 32. Accessed on 12 Nov 2022.
- [18] Pooya Khorrami, Thomas Paine, and Thomas Huang. 2015. Do Deep Neural Networks Learn Facial Action Units when Doing Expression Recognition?. In *The IEEE/CVF International Conference on Computer Vision-workshop (ICCVw)*. 19–27.
- [19] Hye-Rin Kim, Yeong-Seok Kim, Seon Joo Kim, and In-Kwon Lee. 2018. Building Emotional Machines: Recognizing Image Emotions through Deep Neural Networks. *IEEE Transactions on Multimedia (TMM)* 20, 11 (2018), 2980–2992.
- [20] Ronak Kosti, Jose Alvarez, Adria Recasens, and Agata Lapedriza. 2019. Context based Emotion Recognition using EMOTIC Dataset. *IEEE Transactions on Pattern Analysis and Machine Intelligence (PAMI)* (2019).
- [21] Alex Krizhevsky, Ilya Sutskever, and Geoffrey E Hinton. 2012. ImageNet Classification with Deep Convolutional Neural Networks. *Advances in Neural Information Processing Systems (NeurIPS)* 25 (2012), 1097–1105.
- [22] Alex Krizhevsky, Ilya Sutskever, and Geoffrey E Hinton. 2017. ImageNet Classification with Deep Convolutional Neural Networks. *Commun. ACM* 60, 6 (2017), 84–90.
- [23] Puneet Kumar and Balasubramanian Raman. 2022. A BERT based Dual-Channel Explainable Text Emotion Recognition system. *Neural Networks* (2022).
- [24] Shan Li and Weihong Deng. 2020. Deep Facial Expression Recognition: A Survey. *IEEE Transactions on Affective Computing (TAC)* (2020).
- [25] Wen Li, Lixin Duan, Dong Xu, and Ivor W Tsang. 2013. Learning with augmented features for supervised and semi-supervised heterogeneous domain adaptation. *IEEE Transactions on Pattern Analysis and Machine Intelligence (TPAMI)* 36, 6 (2013), 1134–1148.
- [26] Jonathan Long, Evan Shelhamer, and Trevor Darrell. 2015. Fully Convolutional Networks for Semantic Segmentation. In *IEEE/CVF conference on Computer Vision and Pattern Recognition (CVPR)*. 3431–3440.
- [27] Patrick Lucey, Jeffrey F Cohn, Takeo Kanade, Jason Saragih, Zara Ambadar, and Iain Matthews. 2010. The Extended Cohn-Kanade Dataset (CK+): A Complete Dataset for Action Unit and Emotion Specified Expression. In *The IEEE/CVF International Conference on Computer Vision and Pattern Recognition-workshops (CVPRw)*. 94–101.
- [28] Jana Machajdik and Allan Hanbury. 2010. Affective Image Classification using Features Inspired by Psychology and Art Theory. In *18th ACM International Conference on Multimedia*. 83–92.
- [29] Sarthak Malik, Puneet Kumar, and Balasubramanian Raman. 2021. Towards Interpretable Facial Emotion Recognition. In *The 12th Indian Conference on Computer Vision, Graphics and Image Processing*. 1–9.
- [30] Joseph A Mikels, Barbara L Fredrickson, Gregory R Larkin, Casey M Lindberg, Sam J Maglio, and Patricia A Reuter-Lorenz. 2005. Emotional Category Data on Images from the International Affective Picture System. *Behavior research methods* 37, 4 (2005), 626–630.
- [31] Shervin Minaee, Mehdi Minaei, and Amirali Abdolrashidi. 2021. Deep-Emotion: Facial Expression Recognition using Attentional Convolutional Network. *MDPI Sensors* 21, 9 (2021), 3046.
- [32] Sinno Jialin Pan and Qiang Yang. 2009. A Survey on Transfer Learning. *IEEE Transactions on Knowledge and Data Engineering* 22, 10 (2009), 1345–1359.
- [33] Robert Plutchik. 2001. The Nature of Emotions. *Journal Storage (JSTOR) Digital Library's American scientist Journal* 89, 4 (2001), 344–350.
- [34] Tianrong Rao, Xiaoxu Li, and Min Xu. 2019. Learning Multi-level Deep Representations for Image Emotion Classification. *Neural Processing Letters* 51 (2019), 2043–2061.
- [35] Tianrong Rao, Min Xu, Huiying Liu, Jinqiao Wang, and Ian Burnett. 2016. Multi-scale Blocks based Image Emotion Classification using Multiple Instance Learning. In *IEEE International Conference on Image Processing (ICIP)*. 634–638.
- [36] Marco Tulio Ribeiro, Sameer Singh, and Carlos Guestrin. 2016. ‘Why Should I Trust You?’ Explaining the Predictions of Any Classifier. In *The 22nd ACM SIGKDD International Conference on Knowledge Discovery and Data Mining (KDD)*. 1135–1144.
- [37] Artem Rozantsev, Mathieu Salzmann, and Pascal Fua. 2018. Residual parameter transfer for deep domain adaptation. In *Proceedings of the IEEE Conference on Computer Vision and Pattern Recognition*. 4339–4348.
- [38] Kate Saenko, Brian Kulis, Mario Fritz, and Trevor Darrell. 2010. Adapting visual category models to new domains. In *European Conference on Computer Vision (ECCV)*. Springer, 213–226.
- [39] Florian Schroff, Dmitry Kalenichenko, and James Philbin. 2015. FaceNet: A unified embedding for face recognition and clustering. In *IEEE/CVF Conference on Computer Vision and Pattern Recognition (CVPR)*. 815–823.
- [40] LS Shapley. 1953. A Value for n-person Games, Contributions to the Theory of Games II.

- [41] Sumit Shekhar, Vishal M Patel, Hien V Nguyen, and Rama Chellappa. 2013. Generalized domain-adaptive dictionaries. In *Proceedings of the IEEE conference on computer vision and pattern recognition*. 361–368.
- [42] Minchul Shin, Munsang Kim, and Dong-Soo Kwon. 2016. Baseline CNN Structure Analysis for Facial Expression Recognition. In *The 25th IEEE International Symposium on Robot and Human Interactive Communication*. 724–729.
- [43] Avanti Shrikumar, Peyton Greenside, and Anshul Kundaje. 2017. Learning Important Features Through Propagating Activation Differences. In *International Conference on Machine Learning (ICML)*. 3145–3153.
- [44] Karen Simonyan and Andrew Zisserman. 2014. Very Deep Convolutional Networks for Large-Scale Image Recognition. *ArXiv preprint arXiv:1409.1556* (2014). Accessed on 12 Nov 2022.
- [45] Chandan Singh, W James Murdoch, and Bin Yu. 2018. Hierarchical Interpretations for Neural Network Predictions. In *The 6th International Conference on Learning Representations (ICLR)*.
- [46] Eric Tjoa and Cuntai Guan. 2020. A Survey on Explainable Artificial Intelligence (XAI): Towards Medical XAI. *IEEE Transactions on Neural Networks and Learning Systems (TNNLS)* (2020).
- [47] Eric Tzeng, Judy Hoffman, Ning Zhang, Kate Saenko, and Trevor Darrell. 2014. Deep domain confusion: Maximizing for domain invariance. *arXiv preprint arXiv:1412.3474* (2014). Accessed on 12 Nov 2022.
- [48] Ayşegül Uçar, Yakup Demir, and Cüneyt Güzeliş. 2016. A New Facial Expression Recognition based on Curvelet Transform and Online Sequential Extreme Learning Machine Initialized with Spherical Clustering. *Springer Neural Computing and Applications (NCAA)* 27, 1 (2016), 131–142.
- [49] Monu Verma, Jaspreet Kaur Bhui, Santosh K Vipparthi, and Girdhari Singh. 2018. EXPERTNet: Exigent Features Preservative Network for Facial Expression Recognition. In *The 11th Indian Conference on Computer Vision, Graphics and Image Processing (ICVGIP)*. 1–8.
- [50] Kelvin Xu, Jimmy Ba, Ryan Kiros, Kyunghyun Cho, Aaron Courville, Ruslan Salakhudinov, Rich Zemel, and Yoshua Bengio. 2015. Show, Attend and Tell: Neural Image Caption Generation with Visual Attention. In *International Conference on Machine Learning (ICML)*. 2048–2057.
- [51] Victoria Yanulevskaya, Jan C van Gemert, Katharina Roth, Ann-Katrin Herbold, Nicu Sebe, and Jan-Mark Geusebroek. 2008. Emotional Valence Categorization using Holistic Image Features. In *The 15th IEEE International Conference on Image Processing (ICIP)*. 101–104.
- [52] Quanzeng You, Jiebo Luo, Hailin Jin, and Jianchao Yang. 2016. Building a large-scale Dataset for Image Emotion Recognition: The Fine Print and Benchmark. In *Conference on Association for the Advancement of AI (AAAI)*.
- [53] Sicheng Zhao, Guiguang Ding, Yue Gao, Xin Zhao, Youbao Tang, Jungong Han, Hongxun Yao, and Qingming Huang. 2018. Discrete Probability Distribution Prediction of Image Emotions with Shared Sparse Learning. *IEEE Transactions on Affective Computing (TAC)* 11, 4 (2018), 574–587.
- [54] Sicheng Zhao and Yue Gao et al. 2014. Exploring Principles-of-art Features for Image Emotion Recognition. In *22nd ACM International Conference on Multimedia*. 47–56.
- [55] Sicheng Zhao, Hongxun Yao, Yue Gao, Rongrong Ji, and G. Ding. 2016. Continuous Probability Distribution of Image Emotions via Multitask Shared Sparse Regression. *IEEE Transactions on Multimedia (TMM)* 19, 3 (2016), 632–645.